TEMPERATURE STRESSES AND DISPLACEMENTS IN PLANE WEDGES

A. N. Reznikov, M. D. Smirnov, and V. V. Basov

Inzhenerno-Fizicheskii Zhurnal, Vol. 12, No. 3, pp. 374–381, 1967

UDC 536.212

The authors present the results of a photoelastic study of the temperature stresses and displacements in plane wedges. The stresses are determined for a heat source of length l placed at the apex of the wedge and at distances l and $2l$ from the apex.

A number of technical problems reduce to the question of finding the thermal stresses in plane wedges. Such problems are encountered in the study of mechanical friction, in metal-working with cutting and abrading tools, etc. The magnitude and distribution of the thermal stresses have a considerable influence on the operating properties of machine parts and tools. Thus, for example, in a number of cases the temperature stresses in cutting tools, together with the mechanical stresses due to external forces, may cause cracking, chipping, and spalling of the cutting edges.

The causes and distribution of thermal stresses in wedges are insufficiently understood. This is because of the serious difficulties facing an analytical or experimental investigation of these stresses.

We have studied the temperature stresses in wedges using heated models made from optically active materials using the photoelastic method described in [1, 2].

We will consider the method of stress determination with reference to the example of a plane wedge (cutting tool). The heat transfer conditions at the surfaces of the wedge are shown schematically in Fig. 1a. A source of uniform intensity q_S simulates heating of the wedge by the chip, and a sink q_0 takes into account heat exchange with the cooling medium in accordance with Newton's law. When heating of the wedge is due to several sources of different intensity, it is convenient to divide the solution of the basic problem into a number of component problems (see Fig. 1b, c, d). The temperature field of Fig. 1a can be represented as the result of superimposing the fields due to sources q_1, q_2, q_3. For simplicity, the continuous variation of the rate of heat transfer along the length of the working surface of the wedge has been replaced by the action of two heat sinks q_2 and q_3 of length l, which is perfectly permissible [3]. The relations between the flux intensities of the basic problem (Fig. 1a) and its components (Fig. 1b, c, d) can be found from an examination of the temperatures at any points on the wedge.

For the basic problem the temperatures at points 1, 2, 3 on the working side of the wedge at the center of segments of length l can be expressed in terms of the temperatures at the same points for the component problems as follows:

$$\Theta(1) = \Theta_{11} - \Theta_{12} - \Theta_{13},$$
$$\Theta(2) = \Theta_{21} - \Theta_{22} - \Theta_{23},$$
$$\Theta(3) = \Theta_{31} - \Theta_{32} - \Theta_{33}. \qquad (1)$$

The temperature on the right side of these equations can be calculated analytically or determined experimentally. Figure 1b, c, d shows graphs of the variation of the dimensionless temperature Θ on the working surface of the wedge obtained by electrical simulation of the temperature fields on an EHDA-9/60 integrator [3, 4].

The transition from dimensionless temperature fields to actual temperatures can be based on the following known [4] relations:

$$\Theta(1) = \frac{q_1 l}{\lambda L_1}\varkappa_{11} - \frac{q_2 l}{\lambda L_2}\varkappa_{12} - \frac{q_3 l}{\lambda L_3}\varkappa_{13},$$
$$\Theta(2) = \frac{q_1 l}{\lambda L_1}\varkappa_{21} - \frac{q_2 l}{\lambda L_2}\varkappa_{22} - \frac{q_3 l}{\lambda L_3}\varkappa_{23},$$
$$\Theta(3) = \frac{q_1 l}{\lambda L_1}\varkappa_{31} - \frac{q_2 l}{\lambda L}\varkappa_{32} - \frac{q_3 l}{\lambda L_3}\varkappa_{33}\ldots \qquad (2)$$

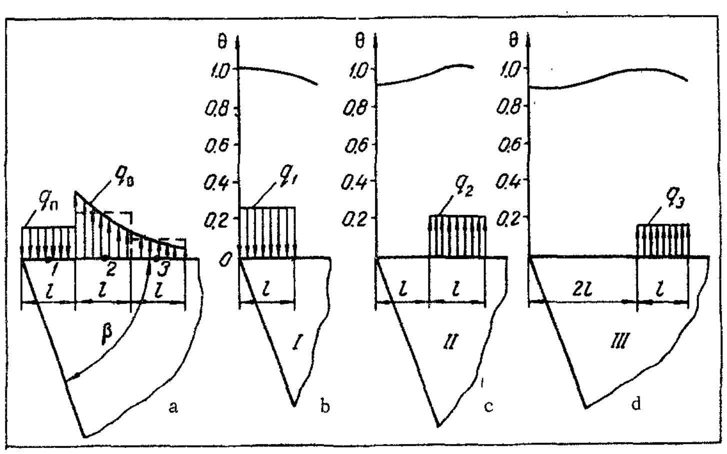

Fig. 1. Diagram illustrating the process of heating of a cutting edge: a) basic problem; b, c, d) its components.

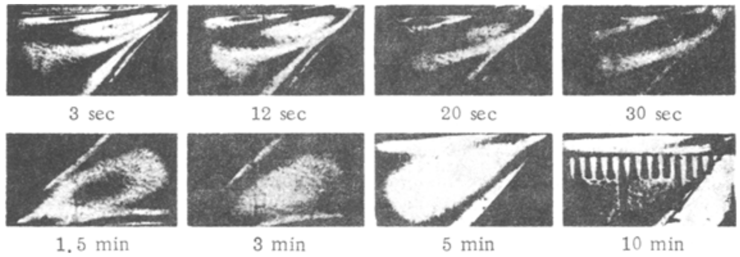

Fig. 2. Stress patterns obtained at different instants of time after beginning to heat a wedge with angle $\beta = 50°$. A source of length l = 14 mm was located at the apex of the wedge. The scale is indicated in the photograph at bottom right.

The values of the quantities $\varkappa_{11}, \varkappa_{12}, \varkappa_{13}, \ldots, \varkappa_{33}$ and L_1, L_2, L_3 are obtained by electrical simulation.

It is clear from (1) and (2) that if the temperatures at points 1, 2, 3 are known, the temperatures for the component problems can be found easily. However, the component problems were simulated separately by the following method.

A model of the wedge was made from the optically sensitive material ED6-M and heated by a special device first on the segment l at the apex of the wedge, and then on segments separated from the apex of the wedge by distances l and $2l$, respectively. Since the variation of temperature over the length of sources q_1, q_2, and q_3 is only slight, as may be seen from Fig. 1b, c, d, the heater can be made so as to ensure a constant temperature on a given contact section between model and heater. In our experiments a constant temperature of 60° C was maintained at the end face of the heater. Up to this temperature the elastic modulus and optical constant of the above-mentioned model material do not vary [1, 2]. On the cooled section of the wedge in separate modeling it is convenient to replace the heat drain to the surrounding medium by heating, since this change subsequently affects only the sign of the stresses. In the process of simulation the stress pattern was observed with a KST-5 polarimeter and photographed with a violet filter (wavelength 435.8 $\mu\mu$). In this way we recorded the variation of the stress pattern from the moment of application of the heater to the moment when the pattern remained almost unchanged over a lengthy heating period (in our experiments 10 min). Figure 2 shows stress patterns for a wedge with an angle $\beta = 50°$ obtained by the method described above at various instants from the beginning of heating. From such stress patterns we constructed curves (Fig. 3) showing the variation of the maximum stresses as a function of heating time and the position of the heater relative to the apex.

It is clear from Fig. 3 that the maximum stresses appear at the moment of application of the heater. The value of the maximum stresses is roughly the same irrespective of the wedge angle β. Extrapolating the stress curves to intersection with the ordinate axis, we obtain approximate values for the maximum stresses σ^* of about 650 N/cm^2.

The maximum stresses σ^* can be calculated theoretically and compared with the experimental results. For a plane wedge [5] the stresses can be found from the formula

$$\sigma^* = -\alpha E \Delta\Theta. \qquad (3)$$

In our experiment $\Delta\Theta = 60° - 22° = 38°$ C (22° C is the temperature of the ambient medium, 60° C is the temperature at the face of the heater). For ED6-M material $\alpha = 52 \cdot 10^6$, $E = 3.3{-}3.51 \cdot 10^5$ N/cm^2.

Substituting the above data in (3), we obtain $\sigma^* = 670$ N/cm^2. As may be seen from this example, the maximum stresses obtained experimentally and calculated theoretically are in good agreement. It can be seen from Fig. 3 that as heating continues the stresses fall. Initially this decrease is very rapid, then it slows somewhat. The stresses are stabilized about 10 min after the beginning of heating. At this point the maximum stresses in the model have fallen by a factor of about 3–5. The smaller the wedge angle and the

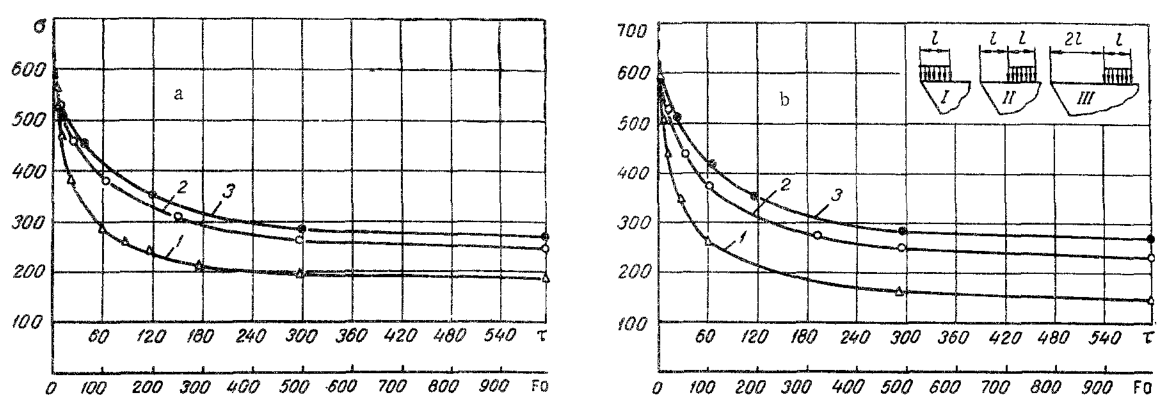

Fig. 3 Maximum stresses σ, N/cm^2, on the heated side of a wedge with wedge angle $\beta = 90°$ (a) and 70° (b). Fo $= a\tau/l^2$ (τ in sec).

closer the heat source to the apex, the greater the fall in maximum stresses. In Fig. 4 we have plotted curves of the normal compressive stresses along the contour of the model for the steady-state temperature field ($\tau > 10$ min). It is clear that the general nature of the stress distribution is roughly the same for all wedge angles. The maximum stresses developed on the heated side of the model. The stress maximum occurs at a certain distance from the apex irrespective of the position of the source.

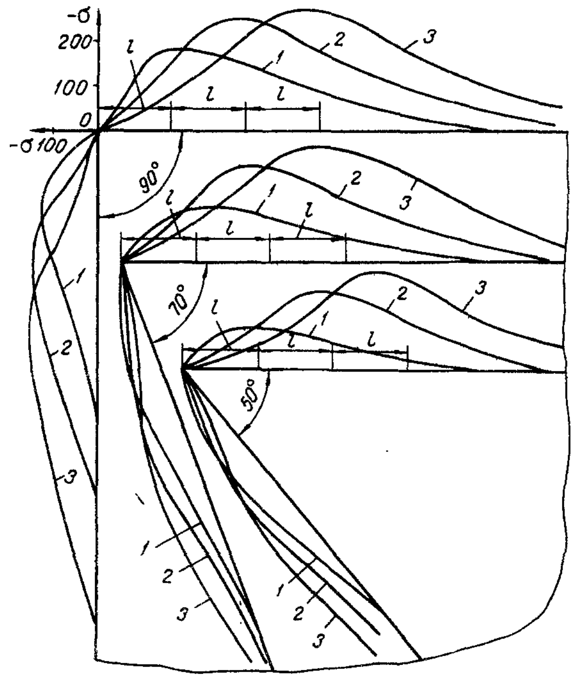

Fig. 4. Normal compressive stresses σ, N/cm^2, along contour of model: 1) heat source at apex, 2) at distance l from apex, 3) at distance $2l$ from apex.

Knowing the temperature stress distribution on the model, we can determine the stresses in real wedges. In the case of a plane state of stress [5] the stress components can be found from the formulas

$$\sigma_x = \frac{\partial^2 \Phi}{\partial y^2}, \quad \sigma_y = \frac{\partial^2 \Phi}{\partial x^2}, \quad \tau_{xy} = -\frac{\partial^2 \Phi}{\partial x \partial y}, \tag{4}$$

where Φ is a stress function satisfying the equation

$$\nabla^4 \Phi + \alpha E \nabla^2 \Theta = 0. \tag{5}$$

Using formulas (4) to determine the stresses in the wedge and the model and taking their ratio, we obtain

$$\sigma_x = \frac{\partial^2 \Phi}{\partial^2 \Phi'} \sigma_x'; \quad \sigma_y = \frac{\partial^2 \Phi}{\partial^2 \Phi'} \sigma_y'; \quad \tau_{xy} = \frac{\partial^2 \Phi}{\partial \Phi'} \tau_{xy}'. \tag{6}$$

We introduce similarity scales for the linear dimensions, temperature, and mechanical characteristics:

$$K_l = \frac{l}{l'}; \quad K_\Theta = \frac{\Theta}{\Theta'}; \quad K_\Phi = \frac{\Phi}{\Phi'};$$

$$K_\alpha = \frac{\alpha}{\alpha'}; \quad K_E = \frac{E}{E'}. \tag{7}$$

The coefficients K_l and K_Θ are independent, and the coefficient K_Φ is determined in terms of the other coefficients by applying Eq. (5) to the wedge and the model. This enables us to obtain

$$K_\Phi = K_\alpha K_E K_\Theta.$$

Accordingly, we can rewrite relations (6) in the form

$$\sigma_x = K_\alpha K_E K_\Theta \sigma_x', \quad \sigma_y = K_\alpha K_E K_\Theta \sigma_y',$$

$$\tau_{xy} = K_\alpha K_E K_\Theta \tau_{xy}'. \tag{8}$$

If we substitute in (8) the values of the mechanical characteristics and the heating temperature of the model (in our case $\Theta = 60°$ C, $\alpha = 52 \cdot 10^6$, $E = 3.3$–$3.51 \cdot 10^5$ N/cm^2, we obtain

$$\sigma_x = 0.015 \alpha E \Theta \sigma_x', \quad \sigma_y = 0.015 \alpha E \Theta \sigma_y',$$

$$\tau_{xy} = 0.015 \alpha E \Theta \tau_{xy}'. \tag{9}$$

Equations (9) can be used to calculate the stresses at the contour of the real wedge for the period of stationary heat transfer.

Figure 5 shows the variation of the stresses along the heated contour in wedges made of different tool materials when the average temperature on the contact length ($0 \le \psi \le 1$) is equal to 570°.

It is clear from Fig. 5 that at the same heating temperature the maximum stresses occur in wedges made of alloy VK8 and the minimum stresses in diamond wedges. The stresses at the instant of contact between the cutting edge and the part are calculated from Eq. (3). For example, for a wedge made of VK8 alloy ($\alpha = 5.5 \cdot 10^{-6}$, $E = 5.4 \cdot 10^7$ N/cm^2) at a temperature $\Theta = 570°$ the maximum stresses will be 1680 N/mm^2. Under similar heating conditions the maximum stresses in diamond cutters ($\alpha = 1.2 \cdot 10^{-6}$, $E = 8.25 \cdot 10^7$ N/cm^2) will be only about 370 N/mm^2. This calculation, without claiming to describe every aspect of the matter, does show that at the same cutting temperatures a diamond tool experiences lower thermal stresses.

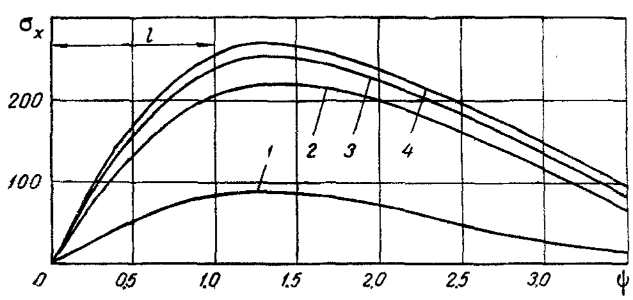

Fig. 5. Normal compressive stresses σ, N/cm^2, along heated contour of wedges ($\psi = x/l$) made of different materials [1) diamond; 2) R18 and T15K6; 3) VK6; 4) VK8]. Wedge angle $\beta = 70°$, heat source on length l.

For other cutting materials the stresses cannot be compared solely on the basis of the individual curves in Fig. 5. In fact, owing to the different thermal conductivities of the tool material under the same cutting conditions different temperatures develop at the working surfaces of cutters made of different materials, which is not taken into account in Fig. 5. A final conclusion concerning the temperature stresses and efficiency of a given wedge material must be based on specific heating conditions with allowance for the thermophysical and mechanical characteristics of the wedge material.

After determining the stresses it is possible to find the displacement of individual points of the model and then calculate the displacement in the real wedge. This is necessary, for example, in order to find the temperature errors due to thermal displacements of the cutting edge.

From known relations for the plane problem

$$\varepsilon_x = \frac{\partial u}{\partial x}; \quad \varepsilon_x = \alpha\Theta + \frac{1}{E}\,\sigma_x,$$

using (8) we find the displacements along the side of the wedge on a segment of length l_1

$$u = K_l K_\Theta \alpha \int_0^{l_1} \Theta'\,dx' - K_l K_\Theta K_\alpha K_E \;\frac{1}{E}\int_0^{l_1} \sigma'_x\,dx', \quad (10)$$

since on the contour $\sigma_y = 0$. In the latter equation the integrands are the areas of the model temperature and stress diagrams.

In order to determine the first integral it is necessary to know the temperature distribution over the model. Using the graphs of Fig. 1, by planimetry we can find the value of $\int_0^{l_1} \Theta' dx'$ for any of the three positions of the heating source. For example, when the source is located at the apex of the wedge (for $\beta = 70°$) the value of this integral is 3650 deg · mm (l_1 was taken equal to $10l$). The second integral can be found by planimetry of the curves in Fig. 4. For example, for a wedge with $\beta = 70°$ and a source located in the first position the value of the integral will be 4.5 N/mm.

As may be seen from Eq. (10), the displacement along the side of the wedge depends on two components, the first of which corresponds to the free temperature expansion of the wedge under the influence of the temperature field, while the second reflects the effect of the temperature stresses preventing the free temperature expansion of the wedge. Calculations based on (10) show that the value of the second term is usually one order smaller than the first. Consequently, in practical calculations it can be neglected and the displacement found from the formula

$$u \approx K_l K_\Theta \alpha \int_0^{l_1} \Theta'\,dx'. \quad (11)$$

NOTATION

$\Theta(1)$, $\Theta(2)$, and $\Theta(3)$ represent temperature at points 1, 2, and 3 on side of wedge, respectively; Θ_{11} and Θ_{12} are the temperatures at point 1 due to sources q_1, q_2, etc., λ is thermal conductivity of wedge material; L_1, L_2, and L_3 are model shape factors for sources located in positions 1, 2, and 3 (for wedge with $\beta = 70°$, $L_1 = 0.184$, $L_2 = 0.209$, $L_3 = 0.210$); $\varkappa_{11}$ is the dimensionless quantity indicating the fraction of the maximum temperature represented by the temperature at point 1 due to source q_1 (the quantities $\varkappa_{12}$, $\varkappa_{13}$, ..., $\varkappa_{33}$ are similarly interpreted); l is the length of heat source; l_1 is the length on which displacement of the wedge is considered; σ are stresses in cutter; σ' are stresses in model; σ^* are maximum stresses; α is the coefficient of linear expansion; E is the modulus of elasticity of first kind; $\Delta\Theta$ is temperature difference between model and ambient medium; σ_x, σ_y, and τ_{xy} are the stress components in wedge; ε_x is the relative strain in direction of x-axis; u is the displacement in direction of x-axis; μ is Poisson's ratio. A prime indicates a model quantity.

REFERENCES

1. G. S. Vardanyan and N. I. Prigorovskii, Izv. AN SSSR, Mekhanika i mashinostroenie, no. 4, 1962.

2. N. I. Prigorovskii, Stresses and Strains in Machine Parts and Assemblies [in Russian], Moscow, 1961.

3. A. N. Reznikov, Heat Transfer and Cooling of Cutting Tools [in Russian], Mashgiz, Moscow, 1963.

4. A. N. Reznikov, A. V. Temnikov, and V. V. Basov, collection: Problems of the Theory and Application of Mathematical Simulation [in Russian], Izd. Sovetskoe radio, Moscow, 1965.

5. E. Melan and H. Parkus, Thermoelastic Stresses Due to Stationary Temperature Fields [Russian translation], Fizmatgiz, Moscow, 1958.

24 June 1966

Kuibyshev Polytechnic Institute, Kuibyshev